Physiologia Plantarum
An International Journal for Plant Biology

Glycine betaine-mediated potentiation of HSP gene expression involves calcium signaling pathways in tobacco exposed to NaCl stress

Meifang Li[a,b], Shangjing Guo[b], Ying Xu[a], Qingwei Meng[a], Gang Li[a] and Xinghong Yang[a,*]

[a]State Key Laboratory of Crop Biology, Shandong Key Laboratory of Crop Biology, Shandong Agricultural University, Taian 271018, China
[b]College of Life Science, Liaocheng University, Liaocheng 252000, China

Correspondence
*Corresponding author,
e-mail: xhyang@sdau.edu.cn

Received 15 December 2012;
revised 22 March 2013

doi:10.1111/ppl.12067

Glycine betaine (GB) can enhance heat tolerance and the accumulation of heat-shock protein (HSP) in plants, but the effects of GB on HSP accumulation during salt stress were not previously known. To investigate the mechanism of how GB influences the expression of HSP, wild-type tobacco (*Nicotiana tabacum*) seedlings pretreated with exogenous GB and *BADH*-transgenic tobacco plants that accumulated GB in vivo were studied during NaCl stress. A transient Ca^{2+} efflux was observed in the epidermal cells of the elongation zone of tobacco roots after NaCl treatment for 1–2 min. After 24 h of NaCl treatment, an influx of Ca^{2+} was observed; a low concentration of GB significantly increased NaCl-induced Ca^{2+} influx. GB increased the intracellular free calcium ion concentration and enhanced the expression of the calmodulin (CaM) and heat-shock transcription factor (HSF) genes resulting in potentiated levels of HSPs. Pharmacological experiments confirmed that Ca^{2+} and CaM increased HSFs and HSPs gene expression, which coincided with increased the levels of HSP70 accumulation. These results suggest a mechanism by which GB acted as a cofactor in the NaCl induction of a Ca^{2+}-permeable current. A possible regulatory model of Ca^{2+}-CaM in the signal transduction pathway for induction of transcription and translation of the active HSPs is described.

Introduction

Salt stress limits crop productivity worldwide, and over 6% of land is affected by salinity (Munns and Tester 2008). In response to salt stress, plants activate various signaling pathways, including those involving calcium (Ca^{2+}) such ion channels, receptors and signaling molecules, and genes involved in producing compatible solutes (e.g. osmoprotectants glycine betaine) (Chen and Murata 2008, Reddy et al. 2011) and heat-shock proteins (HSPs) (Kilstrup et al. 1997, Timperio et al. 2008). Accumulated glycine betaine (GB) may maintain cellular osmotic balance (McCue and Hanson 1992), protect membrane functions from high concentrations of Na^+ and Cl^- (Rhodes and Hanson 1993) and stabilize quaternary structures of complex proteins, such as photosystem II (PSII) (Papageorgiou and Murata 1995, Chen and Murata 2011). Exogenous GB application increased

Abbreviations – $[Ca^{2+}]_{cyt}$, cytosolic free calcium concentration; BADH, betaine aldehyde dehydrogenase; CaM, calmodulin; CBL, calcineurin B-like proteins; CPA, cyclopiazonic acid; CPZ, chlorpromazine; Eosin Y, eosin yellow; Eryth-B, erythtosine B; GB, glycine betaine; HSF, heat-shock transcription factor; HSP, heat-shock protein; LSCM, laser scanning confocal microscopy; NMT, non-invasive microelectrode ion flux measuring techniqu; PM, plasma membrane; PSII, photosystem II; qRT-PCR, quantitative real-time polymerase chain reaction; W7, *N*-(6-aminohexyl)-5-chloro-1-naphthalenesulfonamide; WT, wild-type; ΦPSII, actual PSII efficiency.

environmental stress tolerance in plants that were not able to accumulate GB in previous studies (Yang and Lu 2005, 2006, Park et al. 2006, Chen and Murata 2008). Genetically engineered tobacco was established for the biosynthesis of GB in vivo by introducing the betaine aldehyde dehydrogenase (*BADH*) gene into tobacco; this tobacco showed increased tolerance of photosynthesis to salt stress (Yang et al. 2008). Other studies have also shown that the accumulation of GB in vivo due to genetic engineering enhanced salt tolerance in other plants (Gao et al. 2000, Holmström et al. 2000, Prasad et al. 2000, Goel et al. 2011). However, the mechanism by which low levels (μmol rang) of exogenous GB protect PSII function and enzymes is unclear, especially as the overall level of GB accumulation in vivo is low (Yang and Lu 2005, Yang et al. 2008). GB in vitro stabilizes the DNA double helix structure and results in a lower melting temperature (Rajendrakumar et al. 1997). GB can upregulate a series of genes (Einset et al. 2007). Chen et al. (2009) used proteomic analysis to confirm that the exogenous application of GB upregulates many proteins including PSII, Rubisco and superoxide dismutase when plants are subjected to NaCl stress. GB may be operating via an unidentified signal pathway, and further studies are warranted to determine which pathways are active.

Recent studies examining the effects of GB on ion transport systems in plants have predominantly focused on the influx of K^+ into cells (Cuin and Shabala 2007). Ca^{2+} is involved in nearly all aspects of plant development and participates in many regulatory processes. The importance of Ca^{2+} as a second messenger will be highlighted in this article. In response to NaCl treatment, cytosolic free calcium ($[Ca^{2+}]_{cyt}$) levels were rapidly elevated in previous studies (Lynch et al. 1989, Okazaki et al. 1996, Kiegle et al. 2000). Accordingly, whole-plant $[Ca^{2+}]_{cyt}$ measurements have suggested a direct correlation between the strength of NaCl stress and the magnitude of $[Ca^{2+}]_{cyt}$ elevation (Tracy et al. 2008). $[Ca^{2+}]_{cyt}$ acts as a ubiquitous signal in eukaryotic cells, which activates many downstream intracellular effectors (Dodd et al. 2010, Kudla et al. 2010). This calcium signature forms and disappears by the coordinated action of Ca^{2+} channels, Ca^{2+}-ATPases and Ca^{2+} exchanger isoforms on the plasma membrane (PM) and tonoplast (McAinsh and Pittman 2009). Ca^{2+} influx through Ca^{2+}-permeable channels on the PM is important for triggering $[Ca^{2+}]_{cyt}$ signaling. However, Ca^{2+} release from intracellular stores explains elevated $[Ca^{2+}]_{cyt}$ levels via the calcium-induced calcium release pathway (Pei et al. 2000, Zhang et al. 2007, Wu et al. 2012).

The fast change in $[Ca^{2+}]_{cyt}$ is sensed by several Ca^{2+}-binding proteins or sensors, such as calmodulin (CaM), CaM-like proteins, calcineurin B-like proteins (CBL), CBL-interaction protein kinases and Ca^{2+}-dependent protein kinases (DeFalco et al. 2009). CaM is an important intermediate of calcium-mediated signal transduction (Liu et al. 2003). A change in $[Ca^{2+}]_{cyt}$ is also involved in regulating the binding activity of the heat-shock transcription factor (HSF) to the heat-shock element (Mosser et al. 1990, Li et al. 2004), and the synthesis of HSPs (Charng et al. 2007, Kim and Schöffl 2002). HSPs can act as chaperones of denatured proteins and assist in the translocation and/or degradation of damaged proteins under various stresses (Nollen and Morimoto 2002, Li et al. 2012). Proteomic analysis of salt-stressed tomato seedlings showed that HSPs were 34% of differential expression protein spots and exogenous application of GB resulted in upregulation of some HSPs (Chen et al. 2009). Previous studies have reported involvement of a Ca^{2+}-CaM signaling system in HSP gene expression or HSP synthesis and the order of signal transduction steps during heat stress (Liu et al. 2003, 2008, Zhang et al. 2009, Wu et al. 2012). GB, either applied exogenously or accumulated in vivo in *codA*-transgenic seeds, enhanced the expression of HSPs and improved thermotolerance (Li et al. 2011). It is currently unknown whether GB directly potentiates the expression of HSP genes or if the Ca^{2+}-CaM pathway regulates HSP expression under NaCl stress.

To elucidate the mechanism by which GB influences HSP expression under NaCl stress, the effects of GB on net Ca^{2+} fluxes and $[Ca^{2+}]_{cyt}$ in the elongation zone cells of tobacco root were studied using a non-invasive microelectrode ion flux measuring technique (NMT) and laser scanning confocal microscopy (LSCM). The expression of HSP induced by GB under NaCl stress was also determined using quantitative real-time polymerase chain reaction (qRT-PCR) and western blotting analysis. Our results suggested that GB mediated the expression of HSP involving calcium signaling pathways in tobacco plants under NaCl stress.

Materials and methods

Plant material, salt and GB treatments

Tobacco (*Nicotiana tabacum-K326*) plants were transformed with the *BADH* gene from spinach (*Spinacia oleracea*) that is targeted to the cytosol and chloroplasts. The generation of five homozygous *BADH*-transgenic lines was accomplished as described by Yang et al. (2008). The transgenic line4, which contained the highest levels of GB was used. Transgenic tobacco (T) and wild-type (WT) tobacco seedlings were grown in Hoagland nutrient solution with a photoperiod of 16/8 h light/dark. NaCl (0, 50 and 100 m*M*) and/or GB (0, 5

and 10 m*M*) were dissolved in Hoagland nutrient solution. The 8-day-old tobacco seedlings were treated with GB or other compounds for 1 h, and then exposed to the 50 or 100 m*M* NaCl solution for 24 h. Lanthanum chloride ($LaCl_3$, 1 m*M*) and verapamil (200 μ*M*) were used as Ca^{2+}-permeable channel blockers. Eosin yellow (Eosin Y, 0.5 μ*M*); erythtosine B (Eryth-B, 10 μ*M*) and cyclopiazonic acid (CPA, 50 μ*M*) were used as Ca^{2+}-ATPase metabolic inhibitors in this study. The divalent cation ionophores, Ca^{2+} chelators or CaM antagonists used included A23187 (25 μ*M*), ethylene glycol bis (2-aminoethyl) tetraacetic acid (EGTA) (5 m*M*), *N*-(6-aminohexyl)-5-chloro-1-naphthalenesulfonamide (W7, 300 μ*M*) and chlorpromazine (CPZ, 50 μ*M*). All chemicals were purchased from Sigma (St. Louis, MO, USA). More details and efficient working concentrations referred to Shabala et al. (2011), Nemchinov et al. (2008) and Liu et al. (2003).

GB extraction and quantification

The method developed by Rhodes et al. (1989) was followed. Leaf samples were ground in 2 ml of a mixture of methanol:chloroform:water (12:5:1, v/v/v) at 60°C for 30 min. After centrifugation at 10 000 *g* for 10 min, the aqueous phase was fractionated by ion-exchange chromatography using an Amberlite CG-50 (100–200 mesh, H^+ form; Rohm and Haas Company, Philadelphia, PA, USA) and Dowex 1-X2 (50–100 mesh, Cl^- form; Alfa Aesar Company, Karlsruhe, Germany). The GB fraction was eluted with 6 *M* NH_4OH, dried under a stream of N_2 at 45°C and dissolved in 2 ml of methanol. Betaine in the preliminarily purified extract was analyzed using HPLC (Waters 600) and Millennium Chromatography Manager System Control software on a liquid chromatograph (SCL-10AVP; Shimadzu, Kyoto, Japan) equipped with a Hypersil 10 SCX column.

Measurement of chlorophyll fluorescence, CO_2 assimilation rate and dry weight

Chlorophyll fluorescence was measured with a portable fluorometer FMS2 (Hansatech, King's Lynn, UK). After a dark adaptation period of 30 min, basal non-variable chlorophyll fluorescence level (F_0), maximal fluorescence induction (F_m) and maximal fluorescence level in the light-adapted state (F'_m) were determined according to the experimental protocol of Yang et al. (2008). Using the abovementioned fluorescence parameters, we calculated the actual PSII efficiency using the formula: $(\Phi PSII) = (F'_m - F_s)/F'_m$.

The net CO_2 assimilation rate was measured using a portable photosynthetic system (CIRAS-2, PP Systems, Herts, UK). The measurement was carried out under conditions of concentrated ambient CO_2 (380 μl l^{-1}) and 800 μmol m^{-2} s^{-1} photosynthetic photon flux density. During measurement, relative humidity was maintained at 70% and leaf temperature was set at 24 ± 0.5°C in the leaf chamber.

After 6 weeks of salt and GB treatments, whole plants were collected. The DW of each plant was determined after oven-drying at 80°C for 48 h.

Determination of calcium content

WT and T plants were grown in Hoagland nutrient solution for 6 weeks. After 24 h of NaCl stress, the shoots and roots of the plants were collected separately and dried at 70°C for 2 days prior to tissue ashing and analysis of Ca^{2+} using atomic absorption spectrum (Hitachi Z-8000, Hitachi Ltd., Tokyo, Japan). A minimum of 200 mg dry weight of tissue was used for each tissue sample. Five replicate tissue samples were taken from different pots.

Experimental solutions and protocols for NMT measurements

The net flux of Ca^{2+} was measured by Xuyue-Sci. and Tech. Co. (Beijing, China) (http://www.xuyue.net), using the non-invasive microelectrode ion flux measuring technique (NMT) (BIO-IM, Younger USA LLC, Amherst, MA). Concentration gradients of target ions were measured by moving the ion-selective microelectrode between two positions close to the plant material in a preset excursion with a distance of 20 μm; each cycle was completed in approximately 6 s. Net fluxes of and Ca^{2+} concentrations from the elongation zone of tobacco roots were measured for 15 min using non-invasive ion-selective vibrating microelectrodes. Measurements were completed for three replicate seedlings per treatment. Each sample was floated in measuring solution (0.1 m*M* $CaCl_2$ + 0.1 m*M* KCl + 0.1 m*M* $MgCl_2$ + 0.5 m*M* NaCl +0.2 m*M* Na_2SO_4+ 0.3 m*M* MES, pH 6.0) for at least 30 min before measurement. Data and image acquisition, preliminary processing and control of the electrode positioner and steppermotor-controlled fine focus of the microscope stage were performed using IMFLUX software (Sun et al. 2009). Ionic fluxes were calculated with mageflux, developed by Y. Xu (http://xuyue.net/mageflux).

Measurement of $[Ca^{2+}]_{cyt}$

For measurement of $[Ca^{2+}]_{cyt}$, 1.5 cm long root tissue sections with intact cell layers were obtained from the seedlings. Fluo-3/AM was used as the Ca^{2+}-sensitive fluorescent probe. The tissue was incubated in a medium

containing 10 μ*M* Fluo-3/AM at 24°C in the dark for 2 h prior to imaging. The epidermal root cells were observed using LSCM (Zeiss; LSM510 Meta, Germany). An excitation filter (488 ± 10 nm) and emission filter (530 ± 40 nm) were used in this experiment. The scan mode was XY-T (three dimensional). All image analysis was performed using LSM510 META software.

qRT-PCR analysis

Total RNA was extracted from shoots of 8-day-old seedlings from each treatment using Trizol reagent. Contaminated DNA was removed with RNase-free DNase I. First-strand cDNA synthesis was performed using 4 μg of RNA, oligo (dT) primer and the Qiagen one-step real-time PCR kit (QINGEN, Düsseldorf, Nordrhein Westfalen, German). Primers for gene amplification were designed according to the sequences downloaded from GenBank. The quantitative real-time PCR experiment was carried out at least three times under identical conditions, with the housekeeping gene (actin) as an internal control. Gene expression was determined using the two standard curve method as described by Ramakers et al. (2003) and analyzed by Mx3000P software. The value of WT was set to 1. Details of primers are shown in Table S1.

Immunoblotting of isolated proteins with a HSP70 antibody

After treatment, shoot tissues were ground to a powder in liquid nitrogen. The powder was transferred to a microcentrifuge tube, which contained 1 ml of protein-extraction buffer (20 m*M* Tris–HCl, 1 m*M* EDTA-Na_2, 10 m*M* β-mercaptoethanol, pH 7.5). The homogenate was centrifuged at 14 000 *g* for 10 min at 4°C, and the supernatant was collected as the soluble protein fraction. The amount of protein was determined using the dye-binding assay described by Bradford (1976) with bovine serum albumin as the standard. Proteins in the soluble fraction were separated by sodium dodecyl sulfate polyacrylamide gel electrophoresis (SDS-PAGE), and then electro-blotted onto a polyvinylidene difluoride membrane (Millipore, Boston, MA). Membranes were incubated with an antiserum (1:2000) that had been raised in rabbit against HSP70. Immuno-reactive proteins were detected with peroxidase-conjugated goat antibodies against rabbit IgG (1:5000). Quantitative image analysis of HSP70 was performed using a Tanon Digital Gel Imaging Analysis System (Tanon-4100, Shanghai Tanon Science and Technology Co., Ltd. Shanghai, China).

Statistical analysis

All data obtained was subjected to one-way analysis of variance (ANOVA) using the statistical software SPSS 16.0 and the treatment means were compared by using Duncan's test at $P < 0.05$ or $P < 0.01$. Each data point was mean of five replicates ($n \geq 3$) and was expressed as mean ± standard error (SE).

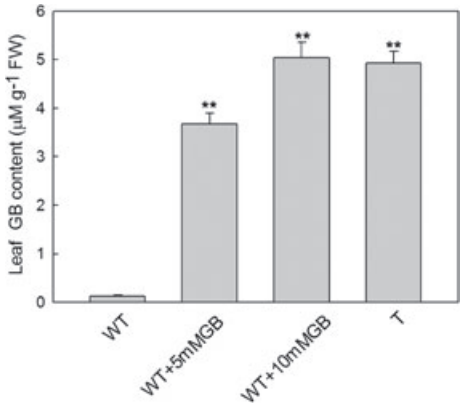

Fig. 1. GB content of WT plants, WT plants pretreated with exogenous GB (5 and 10 m*M*) and *BADH*-transgenic plants. GB content was determined by HPLC. WT: the wild-type tobacco seedling; T: the *BADH*-transgenic seedling. Values represent means ± SE (n = 6). **Significant differences in comparison with the WT at $P < 0.01$.

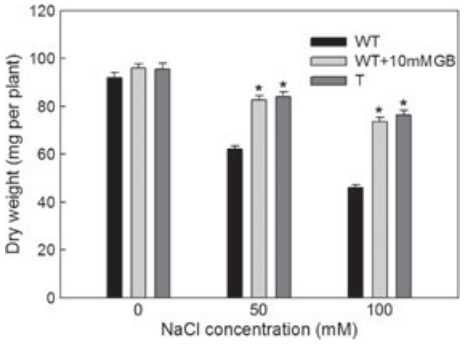

Fig. 2. Changes in dry weight of tobacco seedlings. Exogenous GB uptake in the leaves of tobacco plants following application of GB (10 m*M*) and/or NaCl for 6 weeks. GB treatment was performed by watering the seedlings daily with 300 ml of GB solution (added in the Hoagland solution). WT: the wild-type tobacco seedling; T: the *BADH*-transgenic seedling. Values represent means ± SE (n = 3). *Significant differences in comparison with the WT at $P < 0.05$.

Results

GB accumulation, growth and photosynthetic characteristic of WT and transgenic *BADH* plants

GB could accumulate in transgenic *BADH* plants (T). Exogenous application of GB also increased the GB contents in WT plants (Fig. 1). Growth of tobacco plants was inhibited when exposed to salt stress. The dry weight of plants gradually decreased as the NaCl concentration

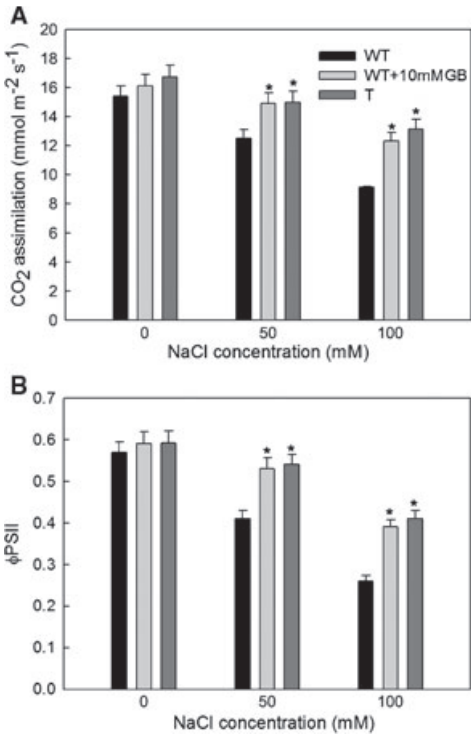

Fig. 3. CO_2 assimilation (A) and actual PSII efficiency (ΦPSII) (B) in tobacco plants under salt stress. WT: the wild-type tobacco seedling; T: the *BADH*-transgenic seedling. Values represent means ± SE (n = 6). *Significant differences in comparison with the WT at $P < 0.05$.

increased, and this decrease was more severe in WT than transgenic plants. Exogenous application of GB also reduced the impact of salt stress on plant growth (Fig. 2).

Photosynthesis is the basis of plant growth and dry mass accumulation. In order to investigate how GB affected dry mass, the CO_2 assimilation rate and the actual PSII efficiency (ΦPSII) of transgenic *BADH* plants and WT plants pretreated with exogenous GB were measured. The CO_2 assimilation rate and ΦPSII of tobacco plants decreased with increasing salt concentration, and the decrease was much greater in WT plants than in transgenic plants and plants pretreated with GB (Fig. 3). These results suggest that salt tolerance is enhanced by GB accumulation as demonstrated through exogenous application and in vivo accumulation in *BADH*-transgenic plants.

GB enhanced NaCl-induced Ca^{2+} influx from tobacco root epidermal cells

Net Ca^{2+} fluxes induced by NaCl were measured by NMT from the tobacco root epidermis. After treatment with NaCl, the Ca^{2+} flux showed a more complex kinetic, switching from a rapidly increased net Ca^{2+} efflux immediately after exposure to NaCl to a steady-state decrease for 15 min and then to an influx state after 24 h (Figs. 4A, C). GB accumulated in vivo (T) reduced the transient Ca^{2+} efflux (Fig. 4A), as did pretreatment with 5 and 10 m*M* GB (data no shown). Figure 4B showed that tobacco roots responded to the NaCl treatment with an immediate large net Ca^{2+} efflux, but increasing the NaCl concentration (50–100 m*M*) did not significantly increase the speed of the outflow of calcium ions. In addition, Ca^{2+}-ATPase metabolic inhibitors (Eosin Y; eryth-B and CPA) had not significantly effect on Ca^{2+} efflux (Fig. 4C).

Net Ca^{2+} flux represents a balance between NaCl-induced Ca^{2+} efflux and influx. After 24 h of salt stress, NaCl-induced influx appeared to dominate over efflux, resulting in a net Ca^{2+} influx. GB, either applied exogenously or accumulated in vivo, potentiated NaCl-induced Ca^{2+} influx in tobacco root epidermal cells after long-time salt stress (Fig. 4D). Pharmacology results showed that $LaCl_3$ rapidly blocked the Ca^{2+} influx, and verapamil had a little effect on Ca^{2+} influx. This indicated that GB may have affected the Ca^{2+}influx through a $LaCl_3$-sensitive channel (Fig. 4E). Ca^{2+}-ATPase metabolic inhibitors (Eosin Y; eryth-B and CPA) slightly affect the net Ca^{2+} influx, indicating GB mainly activated Ca^{2+}-permeable ion channels after 24 h of salt stress (Fig. 4F).

GB potentiated $[Ca^{2+}]_{cyt}$ from tobacco epidermal cells under salt stress for 24 h

To investigate the effect of GB on $[Ca^{2+}]_{cyt}$, the kinetics of change in $[Ca^{2+}]_{cyt}$ were observed at the elongation zone of epidermal cells of 8-day-old tobacco seedling using LSCM. Treatment with 25 µ*M* A23187 (a divalent cation ionophore) and 5 m*M* $CaCl_2$ resulted in a fluorescence intensity of 218.4 (Fig. 5, A_1); whereas, the fluorescence intensity in tissue treated with 5 m*M* EGTA (Ca^{2+} chelator) and 5 m*M* $CaCl_2$ was only 6.9 (Fig. 5, A_2). The fluorescence intensity of WT with non-loaded Fluo-3/AM (Fig. 5, A_3) and WT incubated with 10 µ*M* Fluo-3/AM (Fig. 5, B_1), which were not treated by NaCl were 8.5 and 14.4, respectively, which indicated that autofluorescence (WT without NaCl) was negligible. These results also verified that Fluo-3-fluorescence increase does represent a $[Ca^{2+}]_{cyt}$ increase.

Fluo-3-fluorescence in the cytoplasm was higher in WT with NaCl treatment (Fig. 5, C_1) as compared to WT without NaCl treatment (Fig. 5, B_1). However, a significant increase in $[Ca^{2+}]_{cyt}$ was observed in cells pretreated with GB (Fig. 5, C_2) and transgenic plants cells (T) (Fig. 5, C_3) compared with WT under NaCl stress conditions. The fluorescence intensity increased threefold in

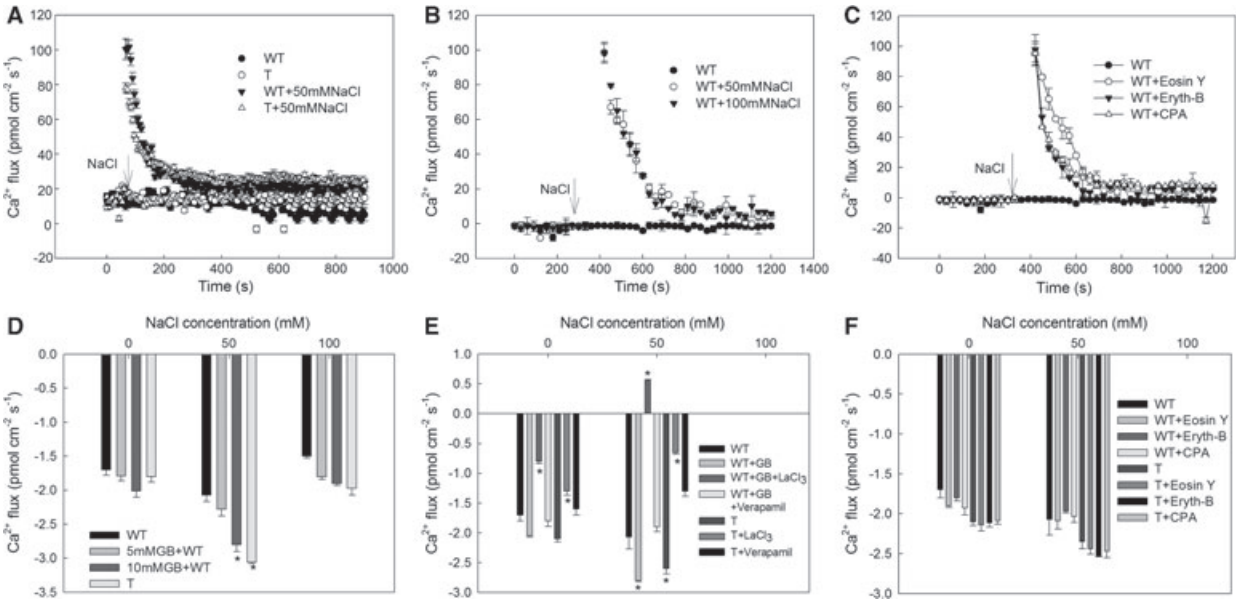

Fig. 4. Effects of GB on the NaCl-induced Ca^{2+} fluxes in the elongation zone of 8-day-old tobacco roots (negative ion flux indicates influx; positive ion flux indicates efflux). Transient Ca^{2+} (A, B and C) flux kinetics from the root cells in response to NaCl treatment are shown. The steady-state flux profile of Ca^{2+} (D, E and F) was examined by continuous flux recording (15–20 min) after 24 h of salt stress. The mean flux values during the measuring periods are shown in the panels. WT: the wild-type tobacco seedling; T: the *BADH*-transgenic seedling. +: introduction of drugs. Fluxes were plotted as the mean ± SE ($n \geq 3$). *Significant differences in comparison with the WT at $P < 0.05$.

both cells of WT with 10 m*M* GB application and in transgenic plants (T) (Fig. 5D), which indicated that GB enhanced $[Ca^{2+}]_{cyt}$ of tobacco epidermal cells, which is consistent with the results of Ca^{2+} influx in Fig. 3C.

GB increased the calcium content of tobacco plants during long-time salt stress

To further investigate whether GB plays a role in Ca^{2+} uptake, the calcium content of WT plants pretreated with GB (WT + GB) and transgenic plants (T) was compared with that of WT plants. GB affected Ca^{2+} acquisition in shoots and roots during long-time NaCl stress, and the calcium content of WT plants pretreated with GB and that of T plants was higher than that of untreated WT plants (Fig. 6). These results were consistent with GB as an activator of Ca^{2+} channels resulting in higher Ca^{2+}influx and $[Ca^{2+}]_{cyt}$ in epidermal cells of tobacco roots during NaCl stress (Figs 4 and 5).

GB influenced the expression of genes under salt stress for 24 h

qRT-PCR analysis showed that *CaM1* had a basal expression level in normal conditions in 8-day-old tobacco seedlings (Fig. 7A). After 24 h of salt stress, *CaM1* gene expression decreased in WT seedlings, while in WT seedlings treated with exogenous GB (WT + GB) and transgenic seedlings (T), the expression of *CaM1* gene was enhanced; EGTA pretreatment decreased *CaM1* expression.

GB enhanced NaCl-induced *HSF/HSPs* gene expression (Fig. 7B, C). Various compounds that affect the Ca^{2+}-CaM signaling system were employed to investigate the role of Ca^{2+}-CaM in upregulating gene expression. *HSFs* levels were elevated in salt stress conditions (Fig. 7B: WT vs WT + NaCl). The expression of *HSF1*and *HSF2* increased during salt stress following treatment with GB (WT + NaCl vs WT + GB + NaCl). Whereas, treatment with the Ca^{2+} chelator EGTA abolished the upregulation by GB (Fig. 7B: WT + GB + NaCl vs WT + GB + EGTA + NaCl). As expected, exogenous GB also significantly potentiated the upregulation of small heat-shock protein gene (*sHSP*) and *HSP70* accumulation (Fig. 7B). Expression of the cytosolic *HSP18p* gene and chloroplast located *HSP26* gene was apparently increased by GB under NaCl stress (Fig. 7B). Transgenic seedlings showed a similar trend for *HSPs* gene expression compared with the respective control (Fig. 7C).

The EGTA treatment caused a remarkable decrease in the level of *CaM1*, *HSF* and *HSP* mRNAs under salt stress conditions (Fig. 7A–C). The expression of *HSF* and *HSPs* decreased in extent with the CaM antagonist (W7 and CPZ), which indicated that GB influenced the expression of genes involving in the Ca^{2+}-CaM pathway.

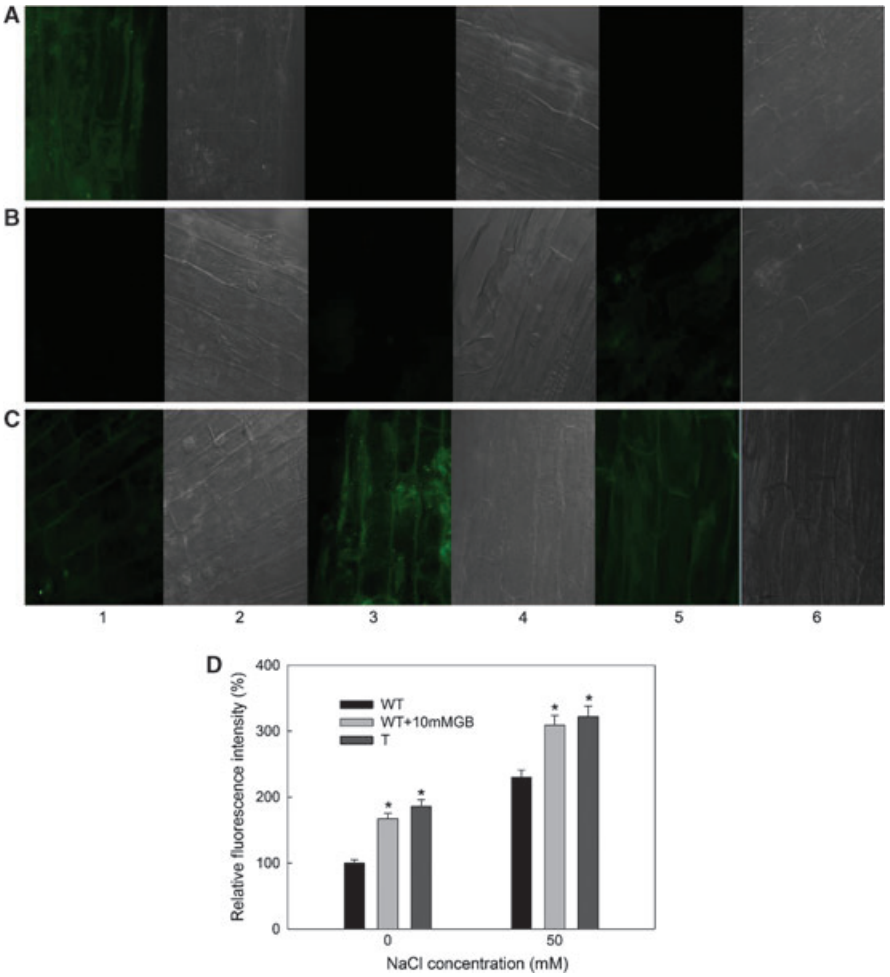

Fig. 5. Pseudocolor LSCM images of the elongation zone of tobacco root cells following different treatments. Roots of 8-day-old green tobacco seedlings were incubated in a medium containing 10 μ*M* Fluo-3/AM at 24°C in the dark for 2 h. One the representative micrograph of the root cells out of four is shown. WT: the wild-type tobacco seedling; T: the *BADH*-transgenic seedling. (A) A_1, Fluo-3-fluorescence in WT treated with 5 m*M* $CaCl_2$ and 25 μ*M* A23187; A_3, autofluorescence in WT non-loaded dye; A_5, Fluo-3-fluorescence in the WT treated with 5 m*M* EGTA; A_2, A_4, and A_6 were the corresponding bright-field image of the cells of A_1, A_3 and A_5, respectively. (B) Pseudocolor images of fluo-3-fluorescence in the tissue of the tobacco root cells without NaCl treatment. B_1, WT; B_3, WT with GB pretreatment; B_5, the T; B_2, B_4 and B_6 are the corresponding bright-field images of the cells of B_1, B_3 and B_5, respectively. (C) Pseudocolor images of fluo-3-fluorescence in the tobacco root cells after NaCl treatment for 24 h. C_1, WT; C_3, WT with GB pretreatment; C_5, T; C_2, C_4 and C_6 were the corresponding bright-field images of the cells of C_1, C_3 and C_5, respectively. (D) The kinetics of $[Ca^{2+}]_{cyt}$ in the elongation zone of tobacco root cells during NaCl stress. The value of fluorescence intensity is an average value obtained by scanning ≥10 cells in three different repeats each experiment. The value of fluorescence intensity WT without NaCl was set to 100%. *Significant differences in comparison with the WT at $P < 0.05$.

GB enhanced the accumulation of HSP70 under salt stress for 24 h

HSP70 expression levels were quantified by western blotting. As noted in Fig. 8, both the accumulation of GB in vivo and exogenously applied GB in WT seedlings enhanced the expression of HSP70. $LaCl_3$, verapamil and EGTA treatment decreased expression levels of HSP70, which suggested GB may enhance expression of heat-shock genes and the accumulation of HSP involved in Ca^{2+} signaling. Western blotting also showed that W7 and CPZ caused a decrease of HSP70, which confirmed further that GB enhanced the synthesis of HSPs involved in the Ca^{2+}-CaM pathway.

Discussion

Exogenously applied GB penetrates into plant leaves quickly and is readily translocated to roots and expanding leaves, remaining unmetabolized in the plant tissue for several weeks (Mäkelä et al. 1996). Thus,

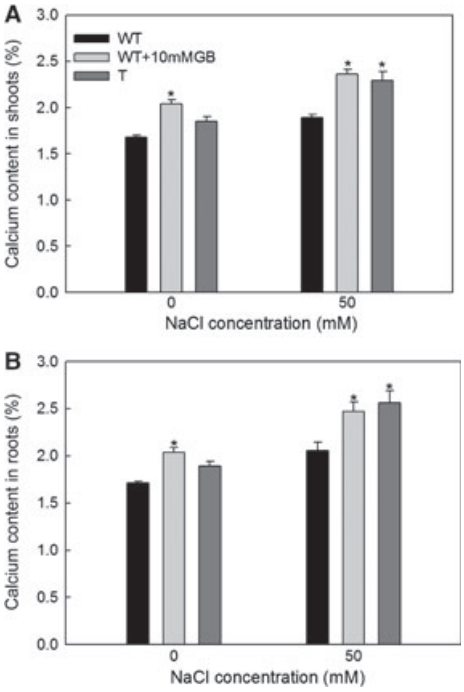

Fig. 6. GB increased calcium contents in shoots and roots compared to WT after application of GB (10 m*M*) and/or NaCl for 6 weeks. (A) GB increased the calcium contents in shoots; (B) GB enhanced calcium contents in roots. WT: the wild-type tobacco seedling; T: the *BADH*-transgenic seedling. Values are the mean ± SE ($n \geq 3$). *Significant differences in comparison with the WT at $P < 0.05$.

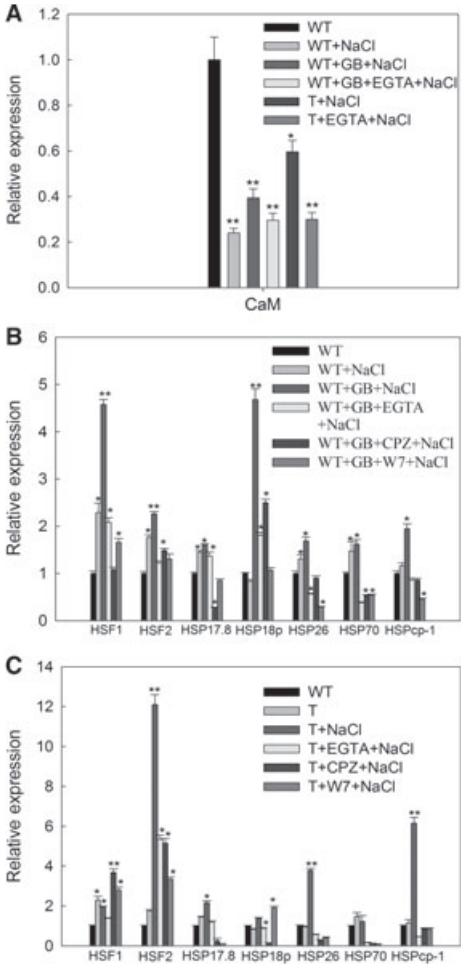

Fig. 7. GB influenced the relative expression of genes compared to WT following different treatments, as revealed by real-time quantitative PCR analysis. (A) GB influenced the relative expression of *CaM1*; (B) GB applied exogenously affected the relative expression of genes; (C) GB accumulated in vivo influenced the relative expression of genes. The average gene activity was obtained from at least fifteen independent shoots, and each assay was repeated three times. The value of WT without NaCl was set to 1. Drugs (5 m*M* EGTA, 50 μ*M* CPZ and 300 μ*M* W7) were introduced to the bath for 1 h before NaCl treatment for 24 h. WT: the wild-type tobacco seedling; T: the *BADH*-transgenic seedling. +: introduction of drugs. Values represent the mean ± SE ($n = 3$). ** and * indicate significant differences in comparison with the WT at $P < 0.01$ and $P < 0.05$, respectively.

being able to compare exogenous application of GB with in vivo accumulation in *BADH*-transgenic plants allows for investigation of the protecting role of GB. GB concentrations were similar in the leaves when 10 m*M* GB was exogenously and in the transgenic *BADH* line (Fig. 1). The dry weight of seedlings gradually decreased as the NaCl concentration increased. GB, either applied exogenously or accumulated in vivo in a *BADH*-transgenic line, increased dry weight (Fig. 2) as a consequence of higher CO_2 assimilation rate and ΦPSII under salinity stress (Fig. 3A, B) which is consistent with results from previous studies (Mäkelä et al. 1999, Lopez et al. 2002, Yang and Lu 2006, Zhang et al. 2011). These results confirm that GB, either applied exogenously or accumulated in vivo in *BADH*-transgenic plants at low concentrations can improve salt tolerance.

Salinity severely affects plant growth due to water stress, ion toxicities and/or ion imbalance (Mahmood et al. 2010, Ashraf et al. 2005). Ca^{2+} transport is impacted by salt stress and a massive Ca^{2+} flux has been reported from cells in response to numerous environmental stresses (Sanders et al. 1999); this flux undoubtedly affects growth, metabolic performance and survival of the plant. It is known that Ca^{2+} influx into the cell is mediated by Ca^{2+}-permeable ion channels that facilitate the rapid movement of Ca^{2+} down its electrochemical gradient (White and Broadley 2003). In contrast, Ca^{2+} movement out of the cell requires active transport mechanisms such as a Ca^{2+} pump. Therefore, the net Ca^{2+} flux measured represents a balance between these two opposing processes. However, high external Na^+ may exchange with Ca^{2+} in the cell wall, which may confound observations of salinity effects on the

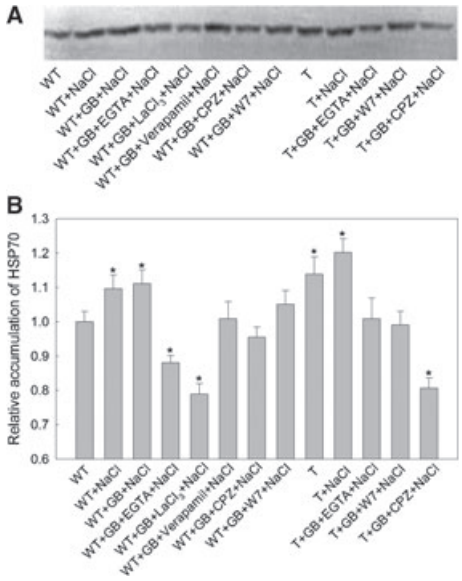

Fig. 8. GB potentiated the accumulation of HSP70 in tobacco shoots following different treatments (measured by western blotting using a rabbit anti-HSP70). (A) Representative western blotting analysis of tobacco shoots; (B) the figure represents relative HSP70 accumulation. Drugs (5 m*M* EGTA, 1 m*M* $LaCl_3$, 200 μ*M* verapamil, 50 μ*M* CPZ and 300 μ*M* W7) were introduced to the bath for 1 h before NaCl treatment for 24 h. WT: the wild-type tobacco seedling; T: the *BADH*-transgenic seedling. +: introduction drugs. Values are the mean ± SE (n = 3). *Significant differences in comparison with the WT at $P < 0.05$.

activity of PM Ca^{2+} transporters. An immediate large net Ca^{2+} efflux was observed with the peak Ca^{2+} efflux (from −1.7 to 95 pmol m^{-2} s^{-1}) at 1–2 min after NaCl treatment started (Fig. 4A). However, long-time salt stress promoted calcium influx in epidermal cells in the root elongation zone (Fig. 4D), confirming previous statements that NaCl-induced changes in $[Ca^{2+}]_{cyt}$ (Okazaki et al. 1996, Cramer and Jones 1996). This trend is also consistent with a previous study by Zepeda-Jazo et al. (2011) characterizing an $OH^{\bullet}$-induced Ca^{2+} flux. Concentrations above 50 m*M* NaCl led to 'saturation' kinetics of the exchangeable cell wall, where Ca^{2+} was replaced by Na^+ and H^+ ions (Shabala and Newman 2000). No significant difference was found in the magnitude of the Ca^{2+} flux response following treatment with 50 and 100 m*M* of NaCl (Fig. 4B), which suggests that the presence of the cell wall was crucial for the NaCl-induced Ca^{2+} effluxes at the tissue level that were observed by Shabala and Newman (2000). In addition, Ca^{2+}-ATPase metabolic inhibitors (Eosin Y; eryth-B and CPA) had not significantly effect on Ca^{2+} efflux (Fig. 4C), which indicated the transient NaCl-induced Ca^{2+} efflux was not mainly outflows of calcium efflux systems. Hence, the transient outflows of calcium were likely produced by the cell-wall cation exchange. Ca^{2+} influx was essential in epidermal cells of the root elongation zone under salt stress.

One of the most prominent roles of Ca^{2+} is as a signal transduction element, and the concentration of $[Ca^{2+}]_{cyt}$ is critically important to control many cell responses. In resting cells, the concentration of $[Ca^{2+}]$cyt is lower than 100 n*M*, while Ca^{2+} concentrations in both apoplast and intracellular stores (e.g. endoplasmic reticulum and vacuole) are up tenfold to at least micromolar level (Allen et al. 1995). Ca^{2+} must be maintained at submicromolar level (100–600 n*M*) in the cytosol, as it precipitates phosphate, the energy currency of the cell (Clapham 1995). An important finding reported herein is that GB, when applied exogenously or accumulated in vivo in transgenic seedlings, enhanced NaCl-induced Ca^{2+} influx from tobacco root epidermal cells (Fig. 4D) and affected $[Ca^{2+}]_{cyt}$ in the tobacco epidermal root cells (Fig. 5) after 24 h of salt stress. $[Ca^{2+}]_{cyt}$ increased threefold in cells of transgenic plants (T) than that in WT, which were not upon 300 n*M* and harmless for cells. GB decreased the peak Ca^{2+} efflux, which also confirmed that GB could enhance NaCl-induced Ca^{2+} influx (Fig. 4A).

Multiple channels are involved in Ca^{2+} transport in plant cells (Kudla et al. 2010). A pharmacological approach was used to decipher the contribution of the various transport mechanisms to Ca^{2+} flux. Figure 4E shows that $LaCl_3$ caused a 150% reduction in the magnitude of NaCl-induced Ca^{2+} influx, and verapamil caused a slight reduction, which implied that GB likely mediated the NaCl-induced Ca^{2+} influx mainly through $LaCl_3$-sensitive channels. Ca^{2+}-ATPase metabolic inhibitors (Eosin Y; eryth-B and CPA) slightly affect the net Ca^{2+} influx (Fig. 4F), indicating GB mainly activated Ca^{2+}-permeable ion channels after 24 h of moderate salt stress (50 m*M*). The previous report implicated PM Ca^{2+}-ATPase activation in plant adaptation to osmotic stress (Beffagna et al. 2005). It was assuming an important role of PM Ca^{2+}-ATPase in switching off the signal triggering ROS production (Romani et al. 2004, Bose et al. 2011). GB has a vital role in maintaining the activities of ROS scavenging enzymes (Chen and Murata 2011) to reduce ROS content. PM Ca^{2+}-ATPase activation involves ROS signal, which will be studied in our future work.

GB mainly affected the permeability of Ca^{2+} channels directly resulting in a Ca^{2+} influx (Fig. 4D) and elevated $[Ca^{2+}]_{cyt}$ (Fig. 5). Both the static and dynamic results suggest that GB may affect the Ca^{2+} signal pathways. GB also appeared to increase the Ca^{2+} uptake capability (Fig. 6), which provides new information linking Ca^{2+} uptake and accumulation in shoots during the course of plant growth and development as a possible component

of salt-induced signaling as well as in the heat-shock signal pathway (Liu et al. 2003, Wu et al. 2012). It appears that GB contributes to Ca^{2+} acquisition as part of the normal growth and development of the plant in addition to the Ca^{2+} conductance associated with signaling described by Ma et al. (2008).

In plant cells, the list of messengers used by signaling pathways includes Ca^{2+}, lipids, pH and cyclic GMP (Sanders et al. 1999). No single messenger has been demonstrated to respond to more stimuli than $[Ca^{2+}]_{cyt}$ (Liu et al. 2003). $[Ca^{2+}]_{cyt}$ is sensed by several Ca^{2+}-binding proteins or sensors. CaM is ubiquitous among eukaryotes and is thought to be involved in fundamental cellular processes because of its extraordinary sequence conservation (Lee et al. 2010); it is also a decoder for Ca^{2+} signals induced by NaCl. As a mediator protein of Ca^{2+} signaling, CaM is activated by binding Ca^{2+}, inducing a cascade of regulatory events (Takahashi et al. 2011, Wu et al. 2012). Possible roles of $[Ca^{2+}]_{cyt}$ in CaM gene expression have been documented (Holmström et al. 2000, Wu et al. 2012). After 24 h of salt stress, *CaM1* gene expression decreased in the WT, which indicated transcription of normal genes was hindered. Both exogenous applications of GB and GB accumulation in vivo can increase the expression of *CaM1* gene during salt stress. In addition, the expression decreased to a basal level with EGTA pretreatment (Fig. 7A). These results indicated that the GB-induced enhancement of *CaM1* gene expression depended on $[Ca^{2+}]_{cyt}$ under NaCl stress.

GB can enhance the expression of HSPs (Li et al. 2011). This was especially apparent for the locating chloroplast of HSP, which was rapidly increased in untreated as compared with salt-stressed seedlings (Chen et al. 2009). However, little is known about how GB activates the genes encoding the HSPs. Various studies revealed multiplicity and the complex nature of the plant HSF family (Miller and Miller 2006), which makes the study of the effects of GB on HSPs much more complex. Levels of *HSF1* were elevated in our study during salt stress (Fig. 7B) in agreement with the study by Miller and Miller (2006). GB could increase the expression of *HSF1* and *HSF2* significantly under salt stress; whereas, treatment with EGTA decreased their expression (Fig. 7B), which indicated that the involvement of Ca^{2+} in activation of HSF as reported previously by Mosser et al. (1990). The qRT-PCR analysis also showed that GB increased the mRNA levels of HSP70 and sHSPs (HSP17.8, HSP18p and HSP26) genes in accordance with proteomic analysis of salt-stressed tomato by Chen (Chen et al. 2009), and EGTA decreased the mRNA level (Fig. 7B, C), which confirmed the involvement of Ca^{2+} in HSP synthesis (Charng et al. 2007, Gong et al. 1997).

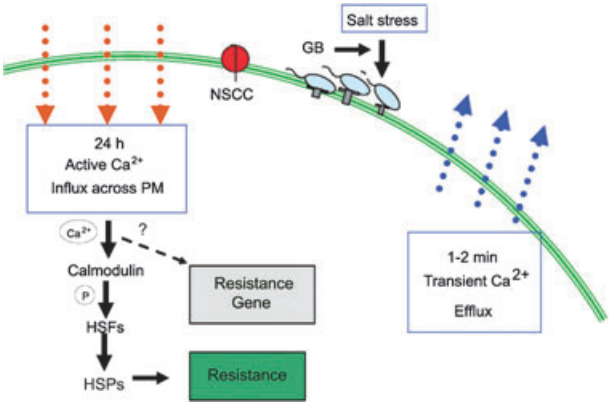

Fig. 9. A putative signaling pathway of GB leads to optimal salt tolerance via Ca^{2+}-CaM and HSP during NaCl stress. GB elevates NaCl induces an increase in $[Ca^{2+}]_{cyt}$ by activating Ca^{2+} channels (NSCC) and triggering Ca^{2+} influx. $[Ca^{2+}]_{cyt}$ activates CaM and promotes the phosphorylation (P) of HSFs. Activated HSFs bind to HSP promoters and induce HSP expression, which contributes to enhance salt tolerance. *Note*: Ca^{2+} affects other possible pathways that are not shown in this model for the sake of clarity to show our results.

The results of this study showed that GB enhanced HSP expression, which was dependent on a Ca^{2+} signal.

Previous work showed that there is a CaM-binding site within maize cytoplasmic HSP70 and that HSP70 binds CaM in a Ca^{2+}-dependent manner (Sun et al. 2000). The conservation of the CaM-binding sequence in cytoplasmic HSP70 family members from eukaryotes implies that the binding of CaM to HSP70 could have an essential biological function. HSP70 is a potential autoregulatory factor that is activated by Ca^{2+} (Kiang et al. 1994). CaM might play a regulatory function during the expression of HSPs by binding directly to cytoplasmic HSP70. When used at the concentrations tested in our study, EGTA, La^{3+}, verapamil, CPZ and W7 did not affect the expression of the monitored genes when no NaCl treatment was applied (data not shown), which was consistent with studies by Liu et al. (2003) and Mosser et al. (1990). These results suggest that HSF is activated directly by a conformational change caused by calcium or by other biochemical conditions. Expression of HSF, sHSP and HSP70 genes was decreased by the CaM antagonists W7 and CPZ (Fig. 7B, C), which suggests that GB increased the expression of HSP involved in the Ca^{2+}-CaM pathway under salt stress. The accumulation of HSP70 decreased with EGTA, $LaCl_3$, verapamil and CaM antagonist (Fig. 8A, B), which further confirms this point.

In conclusion, a putative model was proposed in Fig. 9. NaCl signals are perceived by an unidentified receptor and GB applied exogenously or accumulated in vivo in *BADH*-transgenic plants may act as a cofactor to activate Ca^{2+} channels in the PM or intracellular Ca^{2+}

store membrane resulting in an increase in $[Ca^{2+}]_{cyt}$. This elevated level of $[Ca^{2+}]_{cyt}$ promoted the expression of *CaM1*, which increased the DNA-binding activity of HSF. Activation of HSF initiated transcription and translation of HSP genes, which contributed to salt tolerance of tobacco plants. Other pathways are possible including the regulation of HSF phosphorylation by regulation of CaM-dependent kinase, CDPK, MAPK activity, etc.; future studies may determine definitively which pathways are playing a role.

Acknowledgements – This work was supported by the State Key Basic Research and Development Plan of China (grant number 2009CB118500), the National Natural Sciences Foundation of China (grant number 30970229) and the Research Fund for the Doctoral Program of Higher Education of China (20103702110007).

References

Allen G, Muir S, Sanders D (1995) Release of Ca^{2+} from individual plant vacuoles by both InsP3 and cyclic ADP-ribose. Science 268: 735

Ashraf MY, Akhtar K, Sarwar G, Ashraf M (2005) Role of the rooting system in salt tolerance potential of different guar accessions. Agron Sustain Dev 25: 243–249

Beffagna N, Buffoli B, Busi C (2005) Modulation of reactive oxygen species production during osmotic stress in *Arabidopsis thaliana* cultured cells: involvement of the plasma membrane Ca^{2+}-ATPase and H^{+}-ATPase. Plant Cell Physiol 46: 1326–1339

Bose J, Pottosin II, Shabala SS, Palmgren MG, Shabala S (2011) Calcium efflux systems in stress signaling and adaptation in plants. Front Plant Sci 2: 85

Bradford MM (1976) A rapid and sensitive method for the quantitation of microgram quantities of protein utilizing the principle of protein-dye binding. Anal Biochem 72: 248–254

Charng YY, Liu HC, Liu NY, Chi WT, Wang CN, Chang SH, Wang TT (2007) A heat-inducible transcription factor, HsfA2, is required for extension of acquired thermotolerance in *Arabidopsis*. Plant Physiol 143: 251–262

Chen S, Gollop N, Heuer B (2009) Proteomic analysis of salt-stressed tomato (*Solanum lycopersicum*) seedlings: effect of genotype and exogenous application of glycinebetaine. J Exp Bot 60: 2005–2019

Chen THH, Murata N (2008) Glycinebetaine: an effective protectant against abiotic stress in plants. Trends Plant Sci 13: 499–505

Chen THH, Murata N (2011) Glycinebetaine protects plants against abiotic stress: mechanisms and biotechnological applications. Plant Cell Environ 34: 1–20

Clapham DE (1995) Calcium signaling. Cell 80: 259–268

Cramer GR, Jones RL (1996) Osmotic stress and abscisic acid reduce cytosolic calcium activities in roots of *Arabidopsis thaliana*. Plant Cell Environ 19: 1291–1298

Cuin YA, Shabala S (2007) Compatible solutes reduce ROS-induced potassium efflux in *Arabidopsis* roots. Plant Cell Environ 30: 875–885

DeFalco TA, Bender KW, Snedden WA (2009) Breaking the code: Ca^{2+} sensors in plant signalling. Biochem J 425: 27–40

Dodd AN, Kudla J, Sanders D (2010) The language of calcium signaling. Annu Rev Plant Biol 61: 593–620

Einset J, Nielsen E, Connolly EL, Bones A, Sparstad T, Winge P, Zhu JK (2007) Membrane-trafficking RabA4c involved in the effect of glycinebetaine on recovery from chilling stress in *Arabidopsis*. Physiol Plant 130: 511–518

Gao M, Sakamoto A, Miura K, Murata N, Sugiura A, Tao R (2000) Transformation of Japanese persimmon (*Diospyros kaki* Thunb.) with a bacterial gene for choline oxidase. Mol Breed 6: 501–510

Goel D, Singh AK, Yadav V, Babbar SB, Murata N, Bansal KC (2011) Transformation of tomato with a bacterial codA gene enhances tolerance to salt and water stresses. J Plant Physiol 168: 1286–1294

Gong M, Li Y-J, Dai X, Tian M, Li Z-G (1997) Involvement of calcium and calmodulin in the acquisition of heat-shock induced thermotolerance in maize seedlings. J Plant Physiol 150: 615–621

Holmström KO, Somersalo S, Mandal A, Palva TE, Welin B (2000) Improved tolerance to salinity and low temperature in transgenic tobacco producing glycine betaine. J Exp Bot 51: 177–185

Kiang JG, Carr FE, Burns MR, McClain DE (1994) HSP-72 synthesis is promoted by increase in $[Ca^{2+}]$i or activation of G proteins but not pHi or cAMP. Am J Physiol 267: 104–114

Kiegle E, Moore CA, Haseloff J, Tester MA, Knight MR (2000) Cell-type-specific calcium responses to drought, salt and cold in the Arabidopsis root. Plant J 23: 267–278

Kilstrup M, Jacobsen S, Hammer K, Vogensen FK (1997) Induction of heat shock proteins DnaK, GroEL, and GroES by salt stress in *Lactococcus lactis*. Appl Environ Microbiol 63: 1826–1837

Kim BH, Schöffl F (2002) Interaction between Arabidopsis heat shock transcription factor 1 and 70 kDa heat shock proteins. J Exp Bot 53: 371–375

Kudla J, Batistič O, Hashimoto K (2010) Calcium signals: the lead currency of plant information processing. Plant Cell 22: 541–563

Lee K, Thorneycroft D, Achuthan P, Hermjakob H, Ideker T (2010) Mapping plant interactomes using literature curated and predicted protein–protein interaction data sets. Plant Cell 22: 997–1005

Li B, Liu HT, Sun DY, Zhou RG (2004) Ca^{2+} and calmodulin modulate DNA-binding activity of maize heat shock transcription factor *in vitro*. Plant Cell Physiol 45: 627–634
Li SF, Li F, Wang JW, Zhang W, Meng QW, Chen THH, Murata N, Yang XH (2011) Glycine betaine enhances the tolerance of tomato plants to high temperature during germination of seeds and growth of seedlings. Plant Cell Environ 34: 1931–1943
Liu HT, Gao F, Li GL, Han JL, Liu DL, Sun DY, Zhou RG (2008) The calmodulin-binding protein kinase 3 is part of heat-shock signal transduction in *Arabidopsis thaliana*. Plant J 55: 760–773
Liu HT, Li B, Shang ZL, Li XZ, Mu RL, Sun DY, Zhou RG (2003) Calmodulin is involved in heat shock signal transduction in wheat. Plant Physiol 132: 1186–1195
Li MF, Ji LS, Yang XH, Meng QW, Guo SJ (2012) The protective mechanisms of CaHSP26 in transgenic tobacco to alleviate photoinhibition of PSII during chilling stress. Plant Cell Rep 31: 1969–1979
Lopez CML, Takahashi H, Yamazaki S (2002) Plant-water relations of kidney bean plants treated with NaCl and foliarly applied glycinebetaine. J Agron Crop Sci 188: 73–80
Lynch J, Polito VS, Läuchli A (1989) Salinity reduces membrane-associated calcium in corn root protoplasts. Plant Physiol 90: 1271–1274
Mahmood T, Iqbal N, Raza H, Qasim M, Ashraf MY (2010) Growth modulation and ion partitioning in salt stressed sorghum (*Sorghum bicolor* L.) by exogenous supply of salicylic acid. Pak J Bot 42: 3047–3054
Mäkelä P, Peltonen-Sainio P, Jokinen K, Pehu E, Setälä H, Hinkkanen R, Somersalo S (1996) Uptake and translocation of foliar-applied glycinebetaine in crop plants. Plant Sci 121: 221–230
Mäkelä P, Konttur M, Pehu E, Somersalo S (1999) Photosynthetic response of drought- and salt-stressed tomato and turnip rape plants to foliar-applied glycinebetaine. Physiol Plant 105: 45–50
Ma W, Smigel A, Tsai Y-C, Braam J, Berkowitz GA (2008) Innate immunity signaling: cytosolic Ca^{2+} elevation is linked to downstream nitric oxide generation through the action of calmodulin or a calmodulin-like protein. Plant Physiol 148: 818–828
McAinsh MR, Pittman JK (2009) Shaping the calcium signature. New Phytol 181: 275–294
McCue KF, Hanson AD (1992) Salt-inducible betaine aldehyde dehydrogenase from sugar beet: cDNA cloning and expression. Plant Mol Biol 18: 1–11
Miller G, Miller R (2006) Could heat shock transcription factors function as hydrogen peroxide sensors in plants? Ann Bot 98: 279–288
Mosser DD, Kotzbauer PT, Sarge KD, Morimoto RI (1990) *In vitro* activation of heat shock transcription factor DNA-binding by calcium and biochemical conditions that affect protein conformation. Proc Natl Acad Sci USA 87: 3748–3752
Munns R, Tester M (2008) Mechanisms of salinity tolerance. Annu Rev Plant Biol 59: 651–681
Nemchinov LG, Shabala L, Shabala S (2008) Calcium efflux as a component of the hypersensitive response of *Nicotiana benthamiana* to *Pseudomonas syringae*. Plant Cell Physiol 49: 40–46
Nollen EAA, Morimoto RI (2002) Chaperoning signaling pathways: molecular chaperones as stress-sensing 'heat shock' proteins. J Cell Sci 115: 2809–2816
Okazaki Y, Kikuyama M, Hiramoto Y, Iwasaki N (1996) Short-term regulation of cytosolic Ca^{2+}, cytosolic pH and vacuolar pH under NaCl stress in the charophyte alga *Nitellopsis obtusa*. Plant Cell Environ 19: 569–576
Papageorgiou GC, Murata N (1995) The unusually strong stabilizing effects of glycine betaine on the structure and function of the oxygen-evolving photosystem II complex. Photosynth Res 44: 243–252
Park E-J, Jeknic Z, Chen THH (2006) Exogenous application of glycinebetaine increases chilling tolerance in tomato plants. Plant Cell Physiol 47: 706–714
Pei Z-M, Murata Y, Benning G, Thomine S, Klusener B, Allen GJ, Grill E, Schroeder JI (2000) Calcium channels activated by hydrogen peroxide mediate abscisic acid signalling in guard cells. Nature 406: 731–734
Prasad KVSK, Sharmila P, Kumar PA, Pardha SP (2000) Transformation of *Brassica juncea* (L.) Czern with bacterial coda gene enhances its tolerance to salt stress. Mol Breed 6: 489–499
Rajendrakumar CS, Suryanarayana T, Reddy AR (1997) DNA helix destabilization by proline and betaine: possible role in the salinity tolerance process. FEBS Lett 410: 201–205
Ramakers C, Ruijter JM, Deprez RHL, Moorman AFM (2003) Assumption-free analysis of quantitative real-time polymerase chain reaction (PCR) data. Neurosci Lett 339: 62–66
Reddy ASN, Ali GS, Celesnik H, Day IS (2011) Coping with stresses: roles of calcium- and calcium/calmodulin-regulated gene expression. Plant Cell 23: 2010–2032
Rhodes D, Hanson AD (1993) Quaternary ammonium and tertiary sulfonium compounds in higher plants. Annu Rev Plant Physiol Plant Mol Biol 44: 357–384
Rhodes D, Rich PJ, Brunk DG, Ju GC, Rhodes JC, Pauly MH, Hansen LA (1989) Development of two isogenic sweet corn hybrids differing for glycinebetaine content. Plant Physiol 91: 1112–1121
Romani G, Bonza MC, Filippini I, Cerana M, Beffagna N, De Michelis MI (2004) Involvement of the plasma membrane Ca^{2+}-ATPase in the short-term response of *Arabidopsis thaliana* cultured cells to oligogalacturonides. Plant Biol 6: 192–200

Sanders D, Brownlee C, Harper JF (1999) Communicating with calcium. Plant Cell 11: 691–706
Shabala S, Newman I (2000) Salinity effects on the activity of plasma membrane H^+ and Ca^{2+} transporters in bean leaf mesophyll: masking role of the cell wall. Ann Bot 85: 681–686
Shabala S, Baekgaard L, Shabala L, Fuglsang A, Babourina O, Palmgren MG, Cuin TA, Rengel Z, Nemchinov LG (2011) Plasma membrane Ca^{2+} transporters mediate virus-induced acquired resistance to oxidative stress. Plant Cell Environ 34: 406–417
Sun J, Chen S, Dai S, Wang R, Li N, Shen X, Zhou X, Lu C, Zheng X, Hu Z, Zhang Z, Song J, Xu Y (2009) NaCl-induced alternations of cellular and tissue ion fluxes in roots of salt resistant and salt-sensitive poplar species. Plant Physiol 149: 1141–1153
Sun XT, Li B, Zhou GM, Tang WQ, Bai J, Sun DY, Zhou RG (2000) Binding of the maize cytosolic hsp70 to calmodulin, and identification of calmodulin-binding site in hsp70. Plant Cell Physiol 41: 804–810
Takahashi F, Mizoguchi T, Yoshida R, Ichimura K, Shinozaki K (2011) Calmodulin-dependent activation of MAP kinase for ROS homeostasis in *Arabidopsis*. Mol Cell 41: 649–660
Timperio AM, Egidi MG, Zolla L (2008) Proteomics applied on plant abiotic stresses: role of heat shock proteins (HSP). J Proteomics 71: 391–411
Tracy FE, Gilliham M, Dodd AN, Webb AAR, Tester M (2008) NaCl-induced changes in cytosolic free Ca^{2+} in *Arabidopsis thaliana* are heterogeneous and modified by external ionic composition. Plant Cell Environ 31: 1063–1073
White PJ, Broadley MR (2003) Calcium in plants. Ann Bot 92: 487–511
Wu HC, Luo DL, Vignols F, Jinn TL (2012) Heat shock-induced biphasic Ca^{2+} signature and OsCaM1-1 nuclear localization mediate downstream signalling in acquisition of thermotolerance in rice (*Oryza sativa* L.). Plant Cell Environ 35: 1543–1557
Yang XH, Liang Z, Wen XG, Lu CM (2008) Genetic engineering of the biosynthesis of glycine betaine leads to increased tolerance of photosynthesis to salt stress in transgenic tobacco plants. Plant Mol Biol 66: 73–86
Yang X, Lu C (2005) Photosynthesis is improved by exogenous glycinebetaine in salt-stressed maize plants. Physiol Plant 124: 343–352
Yang X, Lu C (2006) Effects of exogenous glycinebetaine on growth, CO_2 assimilation, and photosystem II photochemistry of maize plants. Physiol Plant 127: 593–602
Zepeda-Jazo I, Velarde-Buendía AM, Enríquez-Figueroa R, Bose J, Shabala S, Muñiz-Murguía J, Pottosin II (2011) Polyamines interact with hydroxyl radicals in activating Ca^{2+} and K^+ transport across the root epidermal plasma membranes. Plant Physiol 157: 2167–2180
Zhang W, Fan LM, Wu WH (2007) Osmo-sensitive and stretch activated calcium-permeable channels in *Vicia faba* guard cells are regulated by actin dynamics. Plant Physiol 143: 1140–1151
Zhang W, Zhou RG, Gao YJ, Zheng SZ, Xu P, Zhang SQ, Sun DY (2009) Molecular and genetic evidence for the key role of AtCaM3 in heat-shock signal transduction in *Arabidopsis*. Plant Physiol 149: 1773–1784
Zhang N, Si H-J, Wen G, Du H-H, Liu B-L, Wang D (2011) Enhanced drought and salinity tolerance in transgenic potato plants with a *BADH* gene from spinach. Plant Biotechnol Rep 5: 71–77

Supporting Information

Additional Supporting Information may be found in the online version of this article:

Table S1. The sequence of primers for qRT-PCR.

Edited by M. Uemura